

We are IntechOpen, the world's leading publisher of Open Access books Built by scientists, for scientists

6,900

Open access books available

185,000

International authors and editors

200M

Downloads

Our authors are among the

154

Countries delivered to

TOP 1%

most cited scientists

12.2%

Contributors from top 500 universities



WEB OF SCIENCE™

Selection of our books indexed in the Book Citation Index
in Web of Science™ Core Collection (BKCI)

Interested in publishing with us?
Contact book.department@intechopen.com

Numbers displayed above are based on latest data collected.
For more information visit www.intechopen.com



Operating Range Evaluation of RFID Systems

Peter. H. Cole, Zhonghao Hu and Yuexian Wang

*The University of Adelaide
Australia*

1. Introduction

Operating range is one of the most significant criteria in evaluating the performance of RFID systems, especially UHF RFID systems. That is because a longer operating range can create more potential application opportunities and ensure a more reliable performance. The operating range is determined by the whole RFID system design rather than just a part of it. Hence, it is worth doing some analysis to find out the methods for evaluating the operating range and which factors, in an overall system design, may play a key role in improving the operating range. In order to achieve this target, this chapter provides in Section 2 an RFID technology background by explaining some relevant terminologies in the antenna performance. The considerations of designing tag antennas in reality are described in Section 3. Then Section 4 and Section 5 analyse two limitations 1) threshold power in exciting a transponder, and 2) sensitivity of a reader, in achieving a successful communication between the transponder and the reader. Section 6 summarises the existing work in the literature on analysing the operating range of UHF RFID systems. The existing work is based on either theoretical analysis according to the Friis equation or totally experimental analysis in real RFID systems. The experimental analysis is a direct solution but may be expensive in cost and time. The limitations of using the Friis equation are given in Section 7. In order to overcome these limitations, Section 8 provides a novel method for evaluating the operating range of RFID systems via a scattering matrix. Lastly the key factors in designing a long operating range RFID systems are identified in Section 9.

2. Fundamental parameters of antennas and the friis equation

2.1 Power transmission in a tag

Fig. 2 shows a Thevenin equivalent circuit of an antenna in its receiving mode. $Z_{ant} = R_{ant} + jX_{ant}$ is the input impedance of the antenna in which R_{ant} is composed of loss resistance R_l and radiation resistance R_r . The receiving antenna is connected to its load $Z_c = R_c + jX_c$ by a transmission line of which the characteristic impedance is Z_0 . V_{in} is the induced voltage caused by the incident wave. In the diagram the induced voltage is represented by a peak value phasor. The source causes a current represented by a peak value phasor I to circulate in the direction shown through all elements of the circuit.

If the receiving antenna shown in Fig. 2 is a tag antenna, then the load presented to the tag antenna is a chip. In fact, the transmission line between the tag antenna and the chip is very short, hence the antenna output impedance at port AB is nearly the same to the transferred impedance at port $A'B'$. Fig. 1 is thus simplified to Fig. 2, in which the symbols representing

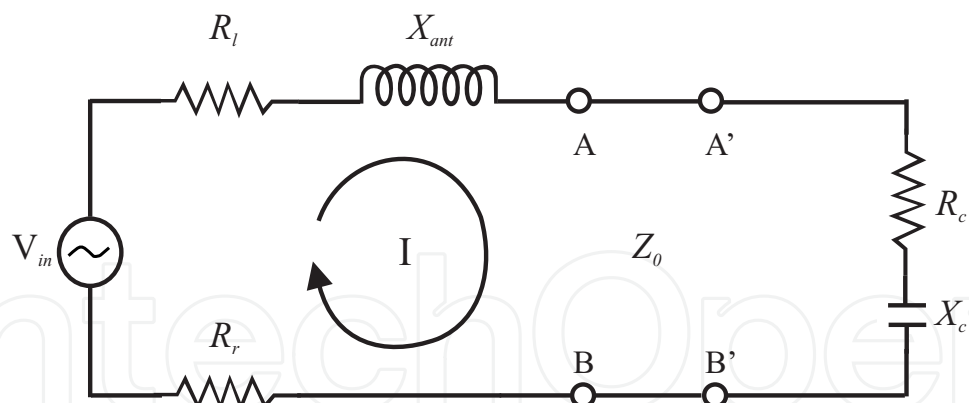


Fig. 1. Thevenin equivalent of a receiving antenna.

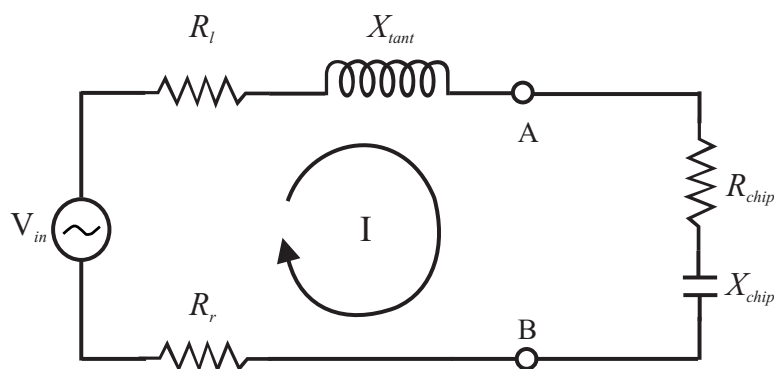


Fig. 2. Thevenin equivalent of a transponder.

the impedance elements are rewritten to keep correspondence with the situation here. $Z_{chip} = R_{chip} + X_{chip}$ is the impedance of the chip presented to the tag antenna. $Z_{tant} = R_{tant} + X_{tant}$ is the tag antenna's output impedance. R_{tant} is composed of loss resistance R_l and radiation resistance R_r .

The phasor representing the circulating current is given by

$$I = \frac{V_{in}}{R_{tant} + R_{chip} + j(X_{tant} + X_{chip})} \quad (1)$$

The power captured by the tag (chip and tag antenna) is expressed as follows

$$P_{tag} = \frac{|I|^2(R_{chip} + R_{tant})}{2} = \frac{|V_{in}|^2(R_{chip} + R_{tant})}{2(R_{tant} + R_{chip})^2 + 2(X_{tant} + X_{chip})^2} \quad (2)$$

The power delivered to the chip is given by

$$P_r^{chip} = \frac{|I|^2 R_{chip}}{2} = \frac{|V_{in}|^2 R_{chip}}{2[(R_{tant} + R_{chip})^2 + (X_{tant} + X_{chip})^2]} \quad (3)$$

The load impedance for maximum power transfer is the complex conjugate of the antenna impedance. Thus in this case

$$R_{chip} = R_{tant} \quad (4)$$

$$X_{chip} = -X_{tant} \quad (5)$$

The total power captured is then $\frac{|V_{in}|^2}{4R_{tant}}$ according to Equation 2. Half of the power is delivered to the load which is the maximum available power $P_A = \frac{|V_{in}|^2}{8R_{tant}}$. The other half is consumed by the antenna in the form of scattered power and ohmic losses. If the antenna is lossless which means that $R_l = 0$ so $R_{tant} = R_r$, the backscattered power is $\frac{|V_{in}|^2}{8R_r}$. When the impedance is unmatched whether or not the antenna is a lossless antenna, the chip can only get part of the maximum available power, the ratio of the power P_r^{chip} delivered to the unmatched load to the maximum available power P_A is then

$$\frac{P_r^{chip}}{P_A} = \frac{4R_{tant}R_{chip}}{(R_{tant} + R_{chip})^2 + (X_{tant} + X_{chip})^2} \quad (6)$$

We can use the identity $|Z_{chip} + Z_{tant}|^2 - |Z_{chip} - Z_{tant}^*|^2 = 4R_{tant}R_{chip}$ to write the result above as

$$\frac{P_r^{chip}}{P_A} = \frac{|Z_{chip} + Z_{tant}|^2 - |Z_{chip} - Z_{tant}^*|^2}{|Z_{chip} + Z_{tant}|^2} = 1 - \left| \frac{Z_{chip} - Z_{tant}^*}{Z_{chip} + Z_{tant}} \right|^2 = 1 - |\theta|^2 \quad (7)$$

where $\theta = \frac{Z_{chip} - Z_{tant}^*}{Z_{chip} + Z_{tant}}$ is defined as the reflection coefficient in many publications (Karthaus and Fischer, 2003; Fuschini et al., 2008; Fuschini et al., 2007), but we notice that the expression of θ here is not analogous to a reflection coefficient as defined in most text books because of the conjugate symbol in the numerator. Hence, we would rather just call it the theta parameter. It has the property that its magnitude squared is the fraction of the available source power that is not delivered to the chip.

Using the circuit of Fig. 2 and our definition of the theta parameter, we may derive the expression for the current I.

$$I = \frac{V_{in}}{2R_{tant}}(1 - \theta) \quad (8)$$

The sum of the powers dissipated within and backscattered from the tag antenna becomes

$$P_{sum}^{tag} = \frac{|I|^2 R_{tant}}{2} = \frac{|V_{in}|^2}{8R_{tant}} |1 - \theta|^2 = P_A |1 - \theta|^2 \quad (9)$$

The backscattered power into the air becomes

$$P_{bs}^{tag} = \frac{|I|^2 R_r}{2} = \frac{|V_{in}|^2}{8R_{tant}} \frac{R_r}{R_{tant}} |1 - \theta|^2 = P_A e_r |1 - \theta|^2 \quad (10)$$

where

P_A = the maximum available power of load,

$e_r = \frac{R_r}{R_{tant}}$ is known as the radiation efficiency.

2.2 Effective area

The power capturing characteristics of a receiving antenna can also be described in terms of effective area, which is defined as the ratio of the available power at the terminals of the receiving antenna to the power flux density of a plane wave incident on the antenna on

condition that the polarisation of the receiving antenna and the impinging wave is matched. In mathematical form, it is shown as Equation 11 (Balanis, 2005).

$$A_e = \frac{P_r}{W_i} \quad (11)$$

where

A_e = effective area (m^2),

P_r = available source power (W),

W_i = power density of incident wave (W/m^2).

2.3 Effective length

The induced voltage V_{in} of the receiving antenna shown in Fig. 2 can also be expressed in terms of the antenna effective length.

In order to provide clarity in the definition of the concept of effective length, we introduce as shown in Fig. 3 the definitions of input current and induced voltage for a general antenna.

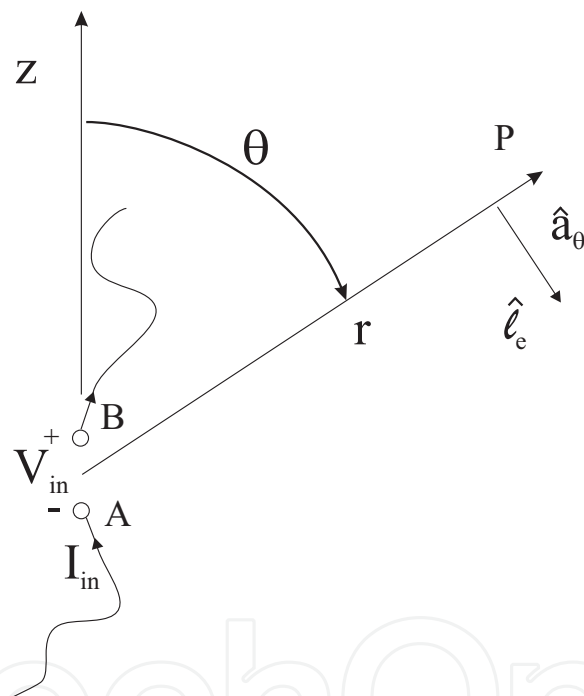


Fig. 3. Coordinate used in the definition of effective length.

The general antenna we consider is excited, when it is driven, by injecting a peak value phasor input current I_{in} at two terminals A,B, shown in Fig. 3. These terminals are also used as the output terminals for the induced voltage V_{in} sensed as shown in Fig. 3 when the antenna receives a signal from an incident field.

Without loss of generality, we place in Fig. 3 terminal B directly above terminal A, and establish a spherical polar co-ordinate system with its origin at the midpoint at the interval AB, and the reference z axis for the polar angle θ in the direction from A to B (other satisfactory co-ordinate systems could be defined, but the one being defined here has the advantage of being defined in a clear way).

It is noted that the antenna need not be a wire antenna. All that is needed is that it have terminals A,B allowing the definition of an input current and of a terminal voltage, and a

co-ordinate system for describing the far field. We note that the far electric field will be in the direction \hat{a}_θ and we will be defining an effective length vector \mathbf{l}_e to be in the same direction as \hat{a}_θ and to have a magnitude to be defined shortly. The value of the effective length vector \mathbf{l}_e is determined by far-zone field \mathbf{E}_a radiated by this antenna (Balanis, 2005).

$$\mathbf{E}_a = -j\eta \frac{k\mathbf{I}_{in}}{4\pi r} \mathbf{l}_e e^{-jkr} \tag{12}$$

where k is the free space propagation constant and η is the characteristic impedance in free space. For a uniform incident electric field represented by a peak value phasor \mathbf{E}^i , using the reciprocity theorem, the voltage V_{in} induced at the terminal of a receiving antenna which is shown in Fig. 2 depends on the same effective length of the antenna as shown in Equation (13) (Balanis, 2005) below.

$$V_{in} = \mathbf{E}^i \cdot \mathbf{l}_e \tag{13}$$

2.4 Gain

Gain is one of the parameters that describe an antenna’s radiating ability. The absolute gain of an antenna (in a given direction) is defined as the ratio of the power density of an antenna radiated to a certain far field point to the power density at the same point which would be radiated by a lossless isotropic emitter. It is expressed as

$$g = \frac{4\pi r^2 W_{rad}}{4\pi r^2 W_{rad}^i} = \frac{W_{rad}}{W_{rad}^i} \tag{14}$$

where g is the gain of the subject antenna, r is the distance from the antenna to a point in far-field zone, which should be larger than $2D^2/\lambda$, (D is the largest dimension of the subject antenna). W_{rad} is the radiation density generated at that point by the subject antenna (Balanis, 2005), W_{rad}^i is the power density of the lossless isotropic emitter. The physical meaning of gain is related to the two factors: (1) directivity D_d and (2) radiation efficiency e_r (Balanis, 2005). Gain can also be expressed in the other form Equation 15 by means of these two factors.

$$g = D_d \times e_r \tag{15}$$

Besides the expression of gain in terms of absolute value as introduced above, another two forms are also widely used. These are dBi and dBd. G_{dBi} is the form of gain which is written in decibels (dB). In mathematical forms, it is shown

$$G_{dBi} = 10 \log_{10} \frac{W_{rad}}{W_{rad}^i} = 10 \log_{10} g \tag{16}$$

Clearly, the reference is still a lossless isotropic emitter. The concept of dBd is similar to dBi. The only difference is that the reference object is changed to a lossless half wavelength dipole antenna instead of a lossless isotropic antenna. Therefore, gain in dBd can be expressed as Equation 17.

$$\begin{aligned} G_{dBd} &= 10 \log_{10} \frac{W_{rad}}{W_{rad}^d} \\ &= 10 \log_{10} \left(\frac{W_{rad}}{W_{rad}^i} \times \frac{W_{rad}^i}{W_{rad}^d} \right) \\ &= 10(\log_{10} g - \log_{10} g_d) \end{aligned} \tag{17}$$

where W_{rad}^d is the radiation density of the half wavelength dipole antenna and g_d is the gain of the dipole which is 1.64. In terms of dBi, it is 2.15dB. Hence, Equation 17 becomes

$$G_{dBd} = G_{dBi} - 2.15\text{dB} \quad (18)$$

2.5 EIRP and ERP

In order to avoid the effects brought by RFID power transmitter to other radio wave devices, many countries impose regulations on the power usage. The radiated power limitation is usually expressed in terms of "EIRP" and "ERP". EIRP and ERP are the acronyms of Equivalent Isotropic Radiated Power and Effective Radiated Power respectively. The regulators do not care about how much power actually is radiated from the reader antenna, although the limitation is described in terms of power. What they really care about is the maximum power density.

The radiation power density of a reader antenna at a distance r can be expressed as Equation 19.

$$W_{rad} = \frac{P_t^{rant} g^{reader}}{4\pi r^2} \quad (19)$$

where P_t^{rant} is the input power to the reader antenna, and g^{reader} is the gain of this antenna. The radiation density caused at the same distance r by a lossless isotropic emitter with input power P_{EIRP} is given in Equation 20.

$$W_{rad} = \frac{P_{EIRP}}{4\pi r^2} \quad (20)$$

The P_{EIRP} that achieves for a lossless isotropic emitter at a given distance the same radiation density as the antenna of gain g^{reader} and input power P_t^{rant} is given by

$$P_t^{rant} = \frac{P_{EIRP}}{g^{reader}} \quad (21)$$

ERP is a similar concept to EIRP, however, the reference emitter is changed to a lossless half wavelength dipole instead of a lossless isotropic emitter. The absolute gain of a lossless half wavelength dipole is 1.64. Therefore,

$$P_t^{rant} = \frac{1.64 P_{ERP}}{g^{reader}} \quad (22)$$

The EIRP and ERP has the following relationship, derived by Equation 21 and Equation 22.

$$P_{EIRP} = 1.64 P_{ERP} \quad (23)$$

2.6 Polarisation

The electric field vector at a point may trace a curve as a function of time. The type of the curve can be used to classify polarisation patterns. Generally, polarisation can be classified into three types which are linear, circular or elliptical polarisation.

When the receiving and transmitting antennas are polarised in the same pattern, the receiving antenna can capture the maximum power emitted from the transmitting one. However, in general, the polarisations of these communicating antennas working in the same system are different, which causes polarisation mismatch.

Polarisation efficiency is involved to evaluate this mismatch. This factor is defined as the

ratio of the actual power received by an antenna to the possible maximum received power which can be accomplished by optimising the matching condition between the polarisation of incident wave and that of receiving antenna. In mathematics, it is expressed as Equation 24 (Balanis, 2005),

$$e_p = \frac{|\mathbf{l}_e \cdot \mathbf{E}^i|^2}{|\mathbf{l}_e|^2 |\mathbf{E}^i|^2} \tag{24}$$

where

\mathbf{l}_e = vector effective length of the receiving antenna which has been introduced in Subsection 2.3,

\mathbf{E}^i = incident electric field.

UHF RFID systems usually adopt linearly polarised antennas as tag antennas because of their low cost and easy fabrication. However, most RFID systems are used to detect mobile items, for example, in the RFID application of supply chains, the cargo on which is mounted a tag will be transported along a supply chain. If the reader antenna is linearly polarised, it is possible that the tag antenna and the reader antenna can be aligned orthogonally to each other. When that happens, the reader will not be able to read or program RFID tags. Hence, RFID reader antennas often adopt circular polarisation to ensure in most of the cases the system can perform correctly. As a result, the polarisation efficiency between a reader antenna in circular polarisation and a tag antenna in linear polarisation is 0.5 i.e. -3dB.

2.7 The Friis transmission equation

After introducing the fundamental parameters for describing an antenna, the Friis transmission equation commonly used in designing and analysing communication systems is given in Equation 25. This equation relates the power delivered to the load of a receiving antenna P_r to the available power P_t from a transmitter which is placed at a distance $r > 2D^2/\lambda$ in free space, where D is the largest dimension of either antenna.

$$P_r = P_t(1 - |\Gamma_t|^2)(1 - |\Gamma_r|^2)g_tg_r(\frac{\lambda}{4\pi r})^2e_p \tag{25}$$

In Equation 25, Γ_t , Γ_r are the reflection coefficients of the transmitting antenna and the receiving antenna respectively, g_t and g_r are the gain of the transmitting and the receiving antenna respectively, as defined in Subsection 2.4, and e_p denotes the polarisation efficiency which is explained in Subsection 2.6.

If the two antenna's impedances are perfectly matched to their source or load and their polarisation is matched as well, an ideal form of Equation 25 is expressed as follows.

$$P_r = P_tg_tg_r(\frac{\lambda}{4\pi r})^2 \tag{26}$$

Equation 25 is an idealised form of the Friis transmission equation. When this equation is applied in analysing RFID systems, a few changes should be made according to the special needs of RFID systems, which are identified in Section 7.

In addition, the factor $(\frac{\lambda}{4\pi r})^2$ which is defined as the path gain describes the dependence of the power received by the transponder on the wavelength and the distance r . Normally, this factor is much less than 1, and we speak of there being a loss. However, this path loss occurs in free space. Most of RFID systems are installed in a building or even a room. Therefore, the path loss in a more complicated environment should be considered before applying it to an RFID system. The evaluation of the in-building path loss has been described in Section 7.

3. Tag antenna design

In Section 2, a few fundamental parameters such as gain, impedance match, polarisation etc, in designing antennas are discussed. Besides those parameters, some other parameters e.g. the antenna size, cost and deployed environment should be considered as well if the antenna is expected to be used in reality. Usually, the tag antenna design is more limited by those parameters required by the reality than the reader antenna design, hence only the tag antenna design is discussed in this section. The parameters required by the reality are discussed respectively in the three following itemisations.

- *Size*
Generally for tag antennas the smaller the better. However, the small size will also affect other factors, such as gain, impedance match and bandwidth. Most of the commercial tags are less than $140\text{mm} \times 40\text{mm}$.
- *Applied environment or attached objects*
Definitely, an RFID system will not be deployed in free space. The applied environment especially when a tag is attached to a metallic object will have a critical impact on the performance of the RFID system because of the metallic boundary conditions. As a result, a solution to this problem is needed before completing an antenna design.
- *Cost*
Generally speaking, a 96-bit EPC inlay (chip and antenna mounted on a substrate) costs from 7 to 15 U.S. cents (RFID Journal, 2010). Low cost tags are always required by the industry for a wide range of applications. One of the possible solutions to reduce the cost significantly is the use of printed electronics, especially printed silicon electronics, which is out of the scope of the work in this chapter. Cole et al. (2010) give more details of the printed electronics and its costs.

Unfortunately and not surprisingly, the factors discussed in this section and the antenna parameters discussed in Section 2 are interacting and usually are not positively related. Some tradeoffs, depending on the system requirements, should be made during the antenna design.

4. Threshold power of a transponder

Chips require a minimum power or voltage to be operated which are called threshold power or threshold voltage. Generally, the threshold power is about $100\mu\text{W}$ (Finkenzeller, 2003) but can be even less down to $16.7\mu\text{W}$ (Karthauss and Fischer, 2003). If the distance between a tag and a reader is too far for the tag to collect more power than the threshold, that tag is unable to be detected. The amount of power or voltage, which can be collected by transponders at a certain distance, depends on the tag antenna design which is briefly discussed in Section 3. Apparently, this threshold is critical to evaluate the reading range of an RFID system and it is definitely decided by the chip IC design. As shown in Figure 4, a typical transponder IC consists of several principal components which are decoder, voltage multiplier, modulator, control logic and memory unit. Each component's power consumption or power transfer efficiency can influence the threshold power. These factors are discussed in the subsections below.

(2005). The task of optimising the factor of θ is out of the scope of the work in this chapter. Hence, it is not discussed further.

4.2 Rectifier efficiency

Once the RF power is received, it will be transmitted to the inside circuit, including voltage multiplier, decoder, control logic and memory units. However, the RF power cannot be used by these components directly and the induced voltage in the terminal of the tag antenna is too small to excite the circuit. As a result, a voltage multiplier is needed to rectify the ac current to dc, and to enlarge the induced ac voltage. This process definitely brings power loss due to the diode and capacitor composing of multiplier. The ratio of dc power produced by the voltage multiplier to the input RF power is called rectifier efficiency. Clearly, threshold power will be increased by a low rectifier efficiency. It was reported that rectifier efficiency ranged from 5-25% (Finkenzeller, 2003). For example, Karthaus and Fischer (2003) achieved a 18% rectifier efficiency. However, with the recent years development of semiconductor technology and circuit design, rectifier efficiency has been improved significantly. Nakamoto et al. (2007) even made the factor to be 36.6%.

4.3 Memory chosen

The threshold power, can be divided into two types: 1) the threshold power for reading and 2) the threshold power for programming. Those two types of threshold power are also related to the memory which is used to store data in the transponder. The data carriers, currently applied, can be categorised into the three types of RAM, EEPROM as well as FeRAM. A comparison among these memories is made below:

- *RAM*
This kind of memory can store data only temporarily. When the voltage supply disappears, the stored data is lost. This form of memory can be used in a passive tag as a temporary information storage when the tag is being read or written. Additionally, it can also be applied in an active tag.
- *EEPROM*
Compared to RAM, EEPROM is a long-term storage memory which can provide reliable data for around ten years (Finkenzeller, 2003). The reading operation with this memory needs a relative low supply voltage which is usually below 5V (Finkenzeller, 2003; Karthaus and Fischer, 2003). Che et al. (2008) even succeed in lowering the threshold voltage to be 0.75V. Moreover, a considerably large voltage (around 17V) is needed to activate the tunnel effect, so that data can be written. Although a charging pump is integrated into the circuit to provide this large voltage and EEPROM is used widely as an RFID tag memory, it still has two serious weakness. Firstly, the power consumption of programming is much larger than that of reading due to the large voltage needed in writing. As a result, the tag integrated with EEPROM cannot be read and written at the same range. Usually, the writing range is only about 20% of the reading range. Secondly, the programming is a time-expensive operation due to the tunneling principle (Nakamoto et al., 2007). In general, it needs 5-10ms for each single-bit or multiple-bit operation.
- *FeRAM*
FeRAM is invented to solve the weaknesses which are faced by EEPROM. The ferroelectric effect is taken advantage of to store data and achieve a balanced power consumption in both reading and programming. In particular, Nakamoto et al. (2007) addressed this

unbalanced reading and writing barriers by employing FeRAM memory. The writing time is also improved to $0.1\mu\text{s}$ (Finkenzeller, 2003; Nakamoto et al., 2007). A 4m operating distance approximately balanced in reading and writing was derived for a 4W EIRP transmitted power. The actual input power of both working modes is nearly the same which are $13\mu\text{W}$ in reading and $15.7\mu\text{W}$ in writing. The writing speed of FeRAM is 100 times faster than that of EEPROM. However, FeRAM has not been widely used in place of EEPROM because FeRAM cells are difficult to combine with CMOS processes, since a high temperature treatment is needed to crystallise the memory materials (PZT or SBT) into ferroelectric phases before the cell is connected to the CMOS (Finkenzeller, 2003; Lung et al., 2004).

Table 1 provides a comparison among the three memories (Finkenzeller, 2003; Fujitsu, 2006).

Comparison parameters	RAM	EEPROM	FeRAM
Size of memory cell	\sim	$\sim 130(\mu\text{m})^2$	$\sim 80(\mu\text{m})^2$
Lifetime in write cycles	∞	10^5	$10^{10} \sim 10^{12}$
Read cycle (ns)	$12 \sim 70$	200	110
Write cycle	$12 \sim 70\text{ns}$	$3 \sim 10\text{ms}$	$0.1\mu\text{s}$
Data write	Overwrite	Erase + Write	Overwrite
Write voltage (V)	3.3	$15 \sim 20$	$2 \sim 3.3$
Energy for Writing	\sim	$100\mu\text{J}$	$0.0001\mu\text{J}$

Table 1. Comparison among RAM, EEPROM and FeRAM.

In conclusion, as long as the modulation mode, the rectifier efficiency, the dc power needed by the chip circuit and the type of memory units are known, the threshold power of transponder can be derived. In particular, Karthaus and Fischer (2003) made a tag which could be read at a distance of 4.5m under only 500mW ERP radiated power. In this case with on-wafer measurements, the rectifier efficiency was established to be 18%, the dc power consumed by the chip circuit was $2.25\mu\text{W}$ ($1.5\mu\text{A}$, 1.5V). As a result, the minimum input RF power for operation is $12.5\mu\text{W}$ ($\frac{2.25\mu\text{W}}{18\%}$). The threshold RF power for reading is the sum of the minimum backscattered power ($4.2\mu\text{W}$) derived by Karthaus and Fischer (2003), and the minimum input RF power ($12.5\mu\text{W}$). However, the threshold power for programming is much larger than that for reading because an EEPROM memory is chosen which choice leads to an unbalanced operating range between reading and programming. The optimisation of all factors discussed in this section is beyond our work, so they will not be discussed further in this chapter.

5. The reader sensitivity

Young (1994) gave the mathematical expression of a general receiver’s sensitivity, and is reproduced as follows.

$$Sen = (S/N)_{min}kTB(NF)$$

(28)

where
 Sen = sensitivity,
 $(S/N)_{min}$ = the minimum signal to noise ratio required to demodulate the replying signal,
 k = Boltzman’s constant,
 B = bandwidth of the receiver,
 NF = noise factor of the receiving equipment,
 T = absolute reference temperature used in the definition of the noise factor.
In the case of an RFID reader the sensitivity can be influenced by several additional factors

including receiver implementation details, receiver gain, communication protocol specifics and interference generated both within the reader and externally by other users of the spectrum. A figure for sensitivity is usually available from the reader manual, and is commonly -70dBm. However, for passive tags the sensitivity is usually good enough for detecting the backscattered signal (Nikitin and Rao, July 2006), and the range is limited by tag excitation, not receiver sensitivity.

6. The literature review on the existing work in evaluating operating range

Significant work has been done in evaluating operating range of RFID systems recent years. Griffin et al. (2006) reported two radio link budgets based on the Friis equation. The first budget links the power received by a chip to the power radiated from a reader antenna. The second budget establishes the relationship between the power received by the reader from the backscattered power of the tag and the power radiated from the reader antenna. The contribution of Griffin et al. (2006) is to add a new factor named as gain penalty in the modified Friis transmission equation. The gain penalty shows to what extent the materials close to the tag can reduce the antenna's gain. However, Griffin et al. (2006) assumes the tag antenna's impedance is always matched to the chip. This is not an accurate assumption because 1) the requirement of the modulation needs at least one state of impedance mismatching, 2) the existence of electro-magnetically sensitive materials in close proximity to the tag will critically vary the output impedance of the tag antenna (Dobkin and Weigand, 2005; Prothro et al., 2006).

Nikitin and Rao (December 2006) introduced a new method in describing and measuring the backscattered power from the tag antenna by means of radar cross section (RCS) based on the Friis transmission equation in free space. Compared with the study by Griffin et al. (2006), the impedance mismatch occurring in the tag and caused by the modulation is considered. The RCS of a meander line dipole antenna in three different situations is investigated by assuming the antenna is placed in free space. The three situations are 1) the antenna is loaded with a chip, 2) the antenna is shorted and 3) the antenna is open circuit. The measurement of the RCS was thus conducted in an anechoic chamber after background subtraction. However, when the tag is deployed in a more complicated environment than in free space, this method is not applicable.

Jiang et al. (2006) proposed another concept *response rate* in evaluating the operating range of an RFID system by experiments. Most of the exciting readers support a "poll" mode, wherein the reader continually scans for the presence of RFID tags. For example, a reader sends N polls within a second, and counts the number of the responses (N_r) from the particularly tag being observed. Therefore, the response rate from that tag is defined as $\alpha = N_r / N$. The larger the response rate is, the more probability the tag will be read. By placing the tag in different positions each time in a complex environment, and counting the response rate of the tag, the readable probability of the tag in various positions can be derived. The optimum position could be found and this optimisation definitely involves the influence of the environment. In addition, people can even place many tags in the complex environment at one time and get the response rate of each tag by experiments. The method not only considers the effects from the environment but also the effects from the mutual coupling among the tags.

Hodges et al. (2007) optimised the position where the tag should be attached on each bottle of wine within a case containing six identical bottles based on a modified response rate test. The test is modified by setting a threshold response rate and attenuating the transmitting power from the reader programmably to meet that threshold response rate. Then the RF margin for

the tag in each location on the wine bottle is tested and the optimum location is determined. According to the discussion above, the existing work is based on either theoretical analysis according to the Friis equation or totally experimental analysis in a real RFID system. The experimental analysis is a direct solution but may be expensive in cost or in time. In addition, the limitation of using the Friis equation is also obvious in that it cannot deal with a complex environment. More details of the Friis equation's limitation in evaluating the operating range of an RFID system are given in Section 7.

Furthermore, the simulation tools such as Ansoft HFSS or CST can accomplish a full wave analysis on the transmission between two antennas or among multiple antennas. A complex environment can be built in the simulation model and considered in the simulation process. The accomplishment of the simulation is definitely dependent on the computing ability of the equipment used. The influences of the environment on the antenna gains and input impedance can be obtained directly, hence people may argue that the Friis equation could still be used combining with the simulation results about the antenna impedance and gain which is similar to what Griffin et al. (2006) did by involving a gain penalty, but the path loss caused in the propagation cannot be obtained directly which is required by the Friis transmission equation. Hence, we totally abandon the Friis equation but turn to evaluating the reading range of an RFID system in any environment by a scattering matrix which takes all the relevant matters into account. More importantly, a scattering matrix can be obtained by both simulation and experiments. This novel method in evaluating the operating range of an RFID system is introduced in Section 8.

7. Interpretation and limitations of the Friis transmission equation in an RFID perspective

In Subsection 2.7, a common form of the Friis transmission equation is given in Equation 25. In addition, Equation 25 is simplified to Equation 26 in an ideal condition. In this section, the physical meaning of each factor in the Friis transmission equation and its usage is interpreted in an RFID perspective. With respect to the radio wave communication between a reader and a passive tag, it is known that the reader firstly interrogates the tag, which is named as forward-link. Then, the tag receives the power from the interrogating wave and makes use of this power to backscatter a signal to the reader, which process is named as backward-link. The Friis transmission equation may be used once in each link. We therefore discuss the use of the Friis transmission equation in the two links respectively and identify its limitations in analysing operating range of an RFID system.

7.1 Forward link

In the forward-link, the reader antenna is in the transmitting mode. Conversely, the tag antenna is in the receiving mode. The Friis transmission equation used in this link is written as follows according to Equation 25.

$$P_r^{chip} = P_t^{reader}(1 - |\Gamma_{rant}|^2)(1 - |\theta|^2)g^{reader}g^{tag}\frac{1}{pl}e_p \tag{29}$$

P_t^{reader} represents the available source power from the reader generator, which has been designed to produce optimum power into a load of real impedance Z_0 and has been connected to the reader antenna by a cable of characteristic impedance Z_0 . P_r^{chip} is the power received by the chip. Γ_{rant} is the reflection coefficient between the reader antenna and the reader which

is expressed in Equation 30a. Z_{rant} is the input impedance of the reader antenna, Z_0 is the characteristic impedance of the transmission line connected to the reader antenna, which is usually 50Ω . θ is the parameter the magnitude squared of which describes the fraction of the available source power not delivered to the tag circuit as defined in Subsection 2.1 and rewritten in Equation 30b in which Z_{chip} is the chip impedance, Z_{tant} is the output impedance of the tag antenna and Z_{tant}^* is conjugate to Z_{tant} . g^{reader} and g^{tag} are the gains of the reader antenna and the tag antenna respectively. The path gain factor $(\frac{\lambda}{4\pi R})^2$ in Equation 25 is changed to be $\frac{1}{pl}$, since the RFID system considered here is not assumed to be operated in free space but a more practical and complex environment.

$$\Gamma_{rant} = \frac{Z_{rant} - Z_0}{Z_{rant} + Z_0} \quad (30a)$$

$$\theta = \frac{Z_{chip} - Z_{tant}^*}{Z_{chip} + Z_{tant}} \quad (30b)$$

The expression of the power input into the reader antenna is given in Equation 31 according to Equation 21.

$$P_t^{rant} = P_t^{reader}(1 - |\Gamma_{rant}|^2) = \frac{P_{EIRP}}{g^{reader}} \quad (31)$$

where P_{EIRP} is the equivalent isotropic radiated power which meaning is given in Subsection 2.5. The involvement of P_{EIRP} is because the maximum power allowed to be radiated is usually described in terms of P_{EIRP} . According to Equation 31, Equation 29 becomes:

$$P_r^{chip} = P_{EIRP}(1 - |\theta|^2)g^{tag}\frac{1}{pl}e_p \quad (32)$$

The maximum value of P_r^{chip} is obtained when P_{EIRP} is set to be maximum which is regulated differently in different countries and regions. To make the tag readable, P_r^{chip} has to be larger than the threshold power for operating the chip, which was discussed in Section 4.

In Equation 7, another form of P_r^{chip} is given in terms of maximum available power P_A and the theta parameter θ , which is rewritten as follows.

$$P_r^{chip} = P_A(1 - |\theta|^2) \quad (33)$$

7.2 Backward link

In the backward-link, the tag antenna is in the transmitting mode. Conversely, the reader antenna is in the receiving mode. The Friis transmission equation used in this link is written as follows.

$$P_r^{reader} = P_{sum}^{tag}(1 - |\Gamma_{rant}|^2)g^{reader}g^{tag}\frac{1}{pl}e_p \quad (34)$$

where P_r^{reader} is the power received by the reader and P_{sum}^{tag} is the sum of the powers dissipated within and backscattered from the tag antenna. The expression of P_{sum}^{tag} has been given in Equation 9 which is rewritten in Equation 35. The path loss factor remains the same as that in Equation 32, since the propagating path in the forward link is the same as in the backward link.

$$P_{sum}^{tag} = P_A|1 - \theta|^2 \quad (35)$$

Solving for P_r^{chip} according to Equation 35 and Equation 33 gives:

$$P_r^{chip} = \frac{1 - |\theta|^2}{|1 - \theta|^2} P_{sum}^{tag} \quad (36)$$

Substituting Equation 36 into Equation 29, another expression of P_{sum}^{tag} is derived.

$$P_{sum}^{tag} = P_t^{reader} (1 - |\Gamma_{rant}|^2) |1 - \theta|^2 g^{reader} g^{tag} \frac{1}{pl} e_p \quad (37)$$

Substituting Equation 37 into Equation 34, then

$$P_r^{reader} = P_t^{reader} [(1 - |\Gamma_{rant}|^2) |1 - \theta| g^{reader} g^{tag} \frac{1}{pl} e_p]^2 \quad (38)$$

Equation 38 establishes the relationship between the power transmitted from the reader P_t^{reader} and the power received by the reader P_r^{reader} after the transmitted wave is backscattered from the tag antenna. P_r^{reader} has to be larger than the sensitivity of the reader which was introduced in Section 5.

According to Equation 31, P_t^{reader} is replaced by $P_{EIRP} / [(1 - |\Gamma_{rant}|^2) g^{reader}]$, Equation 38 becomes:

$$P_r^{reader} = P_{EIRP} (1 - |\Gamma_{rant}|^2) g^{reader} [|1 - \theta| g^{tag} \frac{1}{pl} e_p]^2 \quad (39)$$

7.3 Limitations in implementing the Friis transmission equation

In Subsections 7.1 and 7.2, the power transfer between the transponder and the reader in the forward and backward link is established in Equation 29 and Equation 38 by means of the Friis transmission equation.

However, there are a few limitations in implementing the Friis transmission equations for evaluating the operating range of an RFID system, if the system is deployed in a very complex environment, e.g. 1) when a tag is mounted on a metallic item or a liquid item, or 2) when the testing environment contains a lot of metal reflectors. The reasons of the limitations are given as follows.

1. Far field condition

To implement the Friis transmission equation, the two antennas in communication should be sufficiently far away from each other. The distance between them should be larger than $2D^2/\lambda$, where D is the largest dimension of either antenna, and λ is the free space wavelength at the resonant frequency. However, when an RFID system is placed in the very complex environment as mentioned before, the reader antenna has to be very close to the tag in order to read it. Hence, the distance between them is not sufficient to meet the far field criterion.

2. Gain and impedance variation

In the Friis transmission equation, the gain and input/output impedance of the tag/reader antenna are involved. However, again the RFID system is placed in a very complex environment. The gain pattern and impedance will vary from the intentionally designed values. The effects brought by metals in proximity to a tag antenna to the antenna's output impedance and gain are discussed by Griffin (2006) and Dobkin (2005). It would be possible to investigate those effects by means of simulation or experiments, but that would require effort.

3. Unknown path loss factor

As shown in Equation 31 and Equation 38, path loss factor $\frac{1}{pl}$ is still unknown. If the RFID system is deployed in free space, $\frac{1}{pl}$ is equal to $(\frac{\lambda}{4\pi r})^2$, where r is the distance between the two communicating antennas. Most RFID systems are not deployed in free space but in an in-building environment consisting of many obstacles in the signal propagating path, and the system may be composed of multiple readers and tags. Because of the obstacles in building-environment where an RFID system is deployed, there are more losses brought by path obstruction, reflection, multi-path propagation, absorption and other attenuation effects. In addition, there are also more losses brought by the interaction between the multiple readers and tags.

The analysis of path loss of a dense reader environment was given by Leong (2008). The path loss in dB of a two-antenna RFID system (one tag antenna, one reader antenna) in building is introduced (Rappaport, 2002):

$$PL(\text{dB}) = PL(d_0) + 10 \times n \times \log_{10}\left(\frac{d}{d_0}\right) \quad (40)$$

where d_0 is an arbitrary reference distance; n is a value that depends on the surroundings and building type; d is the distance between the reader antenna and the tag antenna. The reference distance d_0 should be selected to be much smaller than the size of the building, so that the reflection in this small distance is not significant and the path loss in this small distance d_0 can be considered approximately equal to the path loss in free space.

Path loss represented by Equation 40 is a rough evaluation of the general case of an RFID system in building. It does not have the universality of all situations and especially is not suitable for defining the path loss factor in complex environments, e.g. metallic items in near proximity to a tag.

Based on the limitations in implementing the Friis transmission equation in evaluating the operating range of an RFID system, a novel method by means of the scattering matrix is therefore proposed in Section 8.

8. The use of S-parameters in analysing the operating range of RFID systems

8.1 Formula derivation

We consider the two antennas (a reader antenna and a tag antenna) transmission system to be a two port system, as shown in Fig. 5, in which the reader and chip are connected to the reader antenna and the tag antenna by transmission lines of which the characteristic impedance is Z_0 . In Fig. 5, the reader antenna is represented by the two thick lines in the dashed circle for which the input impedance, taking into account the coupling between the antennas, is Z_{rant} , and the tag antenna is represented by the two thin lines in the dashed circle for which the output impedance, taking into account the coupling between the antennas, is Z_{tant} . The resistance of the reader R_{reader} is deliberately designed to be equal to Z_0 (50Ω). In addition, the transmission line between the tag and the chip is very short.

In the following discussion, we will make use of scattering parameters to establish the relationship between the power received by the chip and the power transmitted from the reader antenna. All the values involving voltage and current are represented by peak value phasors.

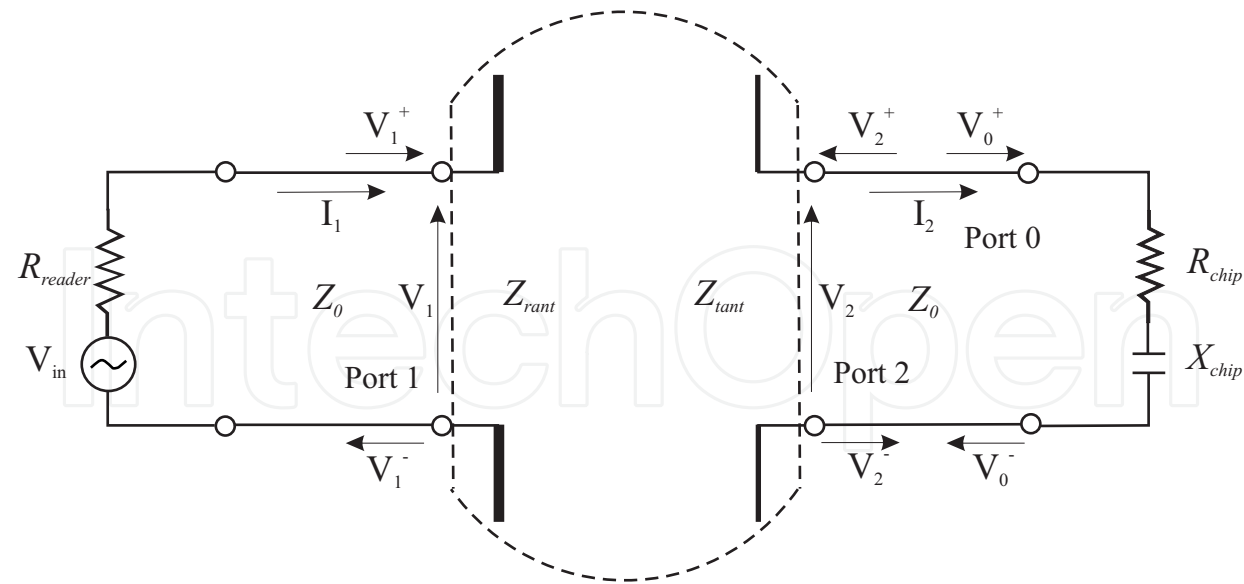


Fig. 5. Two port junction representing coupled antennas in an RFID system.

On the right side of Fig. 5, the voltage V_0 and current I_0 at the load port are expressed in Equation 41.

$$V_0 = V_0^+ + V_0^- \tag{41a}$$

$$I_0 = I_0^+ + I_0^- \tag{41b}$$

The current I_0^+ and I_0^- can also be expressed by the voltage in and out of the load port as shown in Equation 42.

$$I_0^+ = \frac{V_0^+}{Z_0} \tag{42a}$$

$$I_0^- = -\frac{V_0^-}{Z_0} \tag{42b}$$

The ratio of V_0^- / V_0^+ is equal to the reflection coefficient looking into the chip impedance from the terminal of the transmission line, which is written as follows.

$$\frac{V_0^-}{V_0^+} = s_L = \frac{Z_{chip} - Z_0}{Z_{chip} + Z_0} \tag{43}$$

The power received by the chip P_r^{chip} is obtained by Equation 44.

$$P_r^{chip} = \frac{|I_0|^2}{2} R_{chip} = \frac{1}{2} \left| \frac{V_0}{Z_{chip}} \right|^2 R_{chip} = \frac{|V_0^+ + V_0^-|^2 R_{chip}}{2|Z_{chip}|^2} = \frac{|V_0^+|^2 |1 + s_L|^2 R_{chip}}{2|Z_{chip}|^2} \tag{44}$$

As mentioned before, the transmission line between the chip and the tag antenna is very short (its length is nearly zero), hence, $V_0^+ = V_2^-$ and $V_0^- = V_2^+$. Then Equation 43 becomes

Equation 45. In addition, replacing V_0^+ in Equation 44 by V_2^- , Equation 46 is derived.

$$\frac{V_2^+}{V_2^-} = s_L = \frac{Z_{chip} - Z_0}{Z_{chip} + Z_0} \quad (45)$$

$$P_r^{chip} = \frac{|V_2^-|^2 |1 + s_L|^2 R_{chip}}{2|Z_{chip}|^2} \quad (46)$$

Similarly, on the left side of Fig. 5, the voltage V_1 and current I_1 on the port one is expressed in Equation 47.

$$V_1 = V_1^+ + V_1^- \quad (47a)$$

$$I_1 = I_1^+ + I_1^- \quad (47b)$$

The current I_1^+ and I_1^- can also be expressed by the voltage in and out of the port one as shown in Equation 48.

$$I_1^+ = \frac{V_1^+}{Z_0} \quad (48a)$$

$$I_1^- = -\frac{V_1^-}{Z_0} \quad (48b)$$

The ratio of V_1^-/V_1^+ is equal to the reflection coefficient Γ_{rant} which is expressed in Section 7 and rewritten as follows.

$$\frac{V_1^-}{V_1^+} = \Gamma_{rant} = \frac{Z_{rant} - Z_0}{Z_{rant} + Z_0} \quad (49)$$

The power transmitted from the reader antenna P_t^{rant} is obtained by Equation 50.

$$\begin{aligned} P_t^{rant} &= \frac{1}{2} \text{Re}(V_1 \cdot I_1^*) = \frac{1}{2} \text{Re}\left[\frac{1}{Z_0} (V_1^+ + V_1^-) (V_1^+ - V_1^-)^*\right] \\ &= \frac{1}{2} \text{Re}\left[\frac{1}{Z_0} |V_1^+|^2 (1 + \Gamma_{rant})(1 - \Gamma_{rant})^*\right] = \frac{|V_1^+|^2}{2Z_0} (1 - |\Gamma_{rant}|^2) \end{aligned} \quad (50)$$

A scattering matrix can be built according to the simplified two port system shown in Fig. 5 as below.

$$\begin{bmatrix} V_1^- \\ V_2^- \end{bmatrix} = \begin{bmatrix} s_{11} & s_{12} \\ s_{21} & s_{22} \end{bmatrix} \begin{bmatrix} V_1^+ \\ V_2^+ \end{bmatrix} \quad (51)$$

According to the above matrix, the V_1^- and V_2^- can be written into Equation 52.

$$V_1^- = s_{11}V_1^+ + s_{12}V_2^+ \quad (52a)$$

$$V_2^- = s_{21}V_1^+ + s_{22}V_2^+ \quad (52b)$$

Substituting the first of Equation 45 and Equation 49 into Equation 52, solving for V_1^-/V_1^+ and V_2^-/V_1^+ gives

$$\frac{V_1^-}{V_1^+} = \Gamma_{rant} = s_{11} - \frac{s_{12}s_{21}s_L}{s_{22}s_L - 1} \quad (53)$$

$$\frac{V_2^-}{V_1^+} = \frac{s_{21}}{1 - s_{22}s_L} \tag{54}$$

Hence,

$$V_2^- = V_1^+ \frac{s_{21}}{1 - s_{22}s_L} \tag{55}$$

Equation 53 illustrates how the impedance mismatch in the transponder and the testing environment considered in the S parameters affect the reflection occurring between the reader and the reader antenna.

Inserting Equation 55 into Equation 46:

$$P_r^{chip} = \frac{|V_1^+|^2 |s_{21}|^2 |1 + s_L|^2 R_{chip}}{2|1 - s_{22}s_L|^2 |Z_{chip}|^2} \tag{56}$$

Equation 56 demonstrates that the power received by the chip is partially related to $|V_1^+|^2$. The value of $|V_1^+|^2$ can be defined by the combination of Equation 31 and Equation 50 as follows:

$$P_t^{rant} = \frac{|V_1^+|^2}{2Z_0} (1 - |\Gamma_{rant}|^2) = \frac{P_{EIRP}}{g^{reader}} \tag{57}$$

Then Equation 56 becomes:

$$P_r^{chip} = \frac{P_{EIRP}}{g^{reader}} |s_{21}|^2 \frac{R_{chip} Z_0}{|Z_{chip}|^2} \frac{|1 + s_L|^2}{(1 - |\Gamma_{rant}|^2) |1 - s_{22}s_L|^2} \tag{58}$$

In Equation 57, $\frac{|V_1^+|^2}{2Z_0}$ represents the available source power from the reader generator. The product of this power and $(1 - |\Gamma_{rant}|^2)$ denotes the power radiated from the reader antenna. This radiated antenna power can be expressed in terms of P_{EIRP} by multiplying by the gain of the reader antenna g^{reader} . If P_{EIRP} is set to be the maximum power specified by regulations, then Equation 57 tells us that no matter what the reflection between the reader antenna and the transmission line is, the reader antenna can always be made to radiate the same amount of power $\frac{P_{EIRP}}{g^{reader}}$ by adjusting the available source power $\frac{|V_1^+|^2}{2Z_0}$.

Finally, the power received by the chip is represented by means of scattering parameters which can be obtained by the simulation tools or experiments. The complex environment in which the RFID system is deployed can be built in the simulation model and considered in the simulation process. In terms of experiments, the environment is certainly considered. P_{EIRP} is specified by the regulations in different countries and regions separately. In Australia, this factor is equal to 4W or 36dBm as introduced before. g^{reader} is dependent on the reader antenna deployed. s_L can be calculated by Equation 43. The reflection occurring between the reader and the reader antenna represented by Γ_{rant} is caused by the testing environment represented by S parameters and s_L as shown in Equation 53. As a result, P_r^{chip} can be obtained. When P_r^{chip} is less than the threshold power of the chip which is in the order of -10dBm, the reading fails and the maximum reading range can be read in the simulation model or measured directly in experiments. Here, the backward link is not considered since it is concluded (Nikitin, 2006) that the limitation of the reading range of a passive RFID systems mainly comes from the forward link not the backward link because usually the reader's sensitivity is, as mentioned before, low enough to detect the signal from the successfully excited tag.

8.2 Formula validation

In the last subsection, Equation 58 has been derived to calculate the power received by the chip. In this subsection, it is verified by simulation and experiments. However, as mentioned before, to implement Equation 58, the available source power of the reader generator should be adjusted according to Γ_{rant} to keep the radiation power from the reader antenna as P_{EIRP}/g^{reader} . The implemented condition brings some obstacles in the experimental validation, since the available source power of most real reader generators cannot be adjusted arbitrarily. The available source power can only be set stage by stage and the gap between the adjacent stages is large (in our case the gap is 0.1W).

The approach we adopted to solve that problem is to keep the available source power unchanged as P_{EIRP}/g^{reader} which is very easy to achieve by the real reader and leads to:

$$\frac{|V_1^+|^2}{2Z_0} = \frac{P_{EIRP}}{g^{reader}} \quad (59)$$

After substituting Equation 59 into Equation 56:

$$P_r^{chip} = \frac{P_{EIRP}}{g^{reader}} |s_{21}|^2 \frac{R_{chip} Z_0}{|Z_{chip}|^2} \frac{|1 + s_L|^2}{|1 - s_{22} s_L|^2} \quad (60)$$

Equation 60 is more convenient to be used in the form of dB, which is shown in Equation 61.

$$\begin{aligned} P_r^{chip}(\text{dBm}) &= P_{EIRP}(\text{dBm}) - G^{reader}(\text{dBi}) + |S_{21}|(\text{dB}) \\ &\quad + 10 \log_{10} \frac{R_{chip} Z_0}{|Z_{chip}|^2} + 20 \log_{10} \left| \frac{1 + s_L}{1 - s_{22} s_L} \right| \end{aligned} \quad (61)$$

In the following discussion, Equation 58 is verified indirectly by verifying Equation 61 by simulation and experiments. The experiments were conducted by testing the reading range of a self-made tag. The equipment used in the experiments is introduced first.

- *Self-made tag*

The self-made tag shown in Fig. 6 is used. The chip is manufactured by Alien Technology which model is Higgs-2. The chip conforms to the EPCglobal Class 1 Gen 2 specifications. It is implemented in a CMOS process and uses EEPROM memory. The equivalent input impedance of the chip in parallel is shown in Fig. 7(a) in which the parallel resistance R_p is 1500Ω and the parallel capacitance C_p is 1.2pF. Usually, the input impedance of a tag antenna is presented in series. Hence, in order to simplify the analysis, the chip impedance is transformed into a series representation, so Fig. 7(a) becomes Fig. 7(b). At 923MHz which is the centre frequency of UHF RFID band in Australia, the input impedance in series is about $13.6 - j142\Omega$. Hence, Z_{chip} in Equation 61 can be obtained. Typically the threshold power of this chip is -14dBm, but the threshold power is dependent on the manufacturing quality control, the worst could be -11dBm. More details of the chip can be found in the product data sheet (Alien Technology, 2008).

The tag antenna is a meander line dipole antenna fabricated on FR4 board which thickness is 1.6mm and the dielectric constant is 4.4. The footprint of this antenna is 43.8×28.8 (unit mm). The output impedance of this antenna is designed to be approximately conjugate matched to the chip impedance.

The chip is installed on the antenna by electrically conductive adhesive transfer tape

9703 manufactured by 3M (3M, 2007). Currents can pass perpendicularly through the sticky tape. The tape and adhesive material on it will bring losses and chip impedance changes. However, previous experiences with this tape reported by other colleagues in our laboratory indicated that these losses and impedance changes are negligible (NG, 2008).

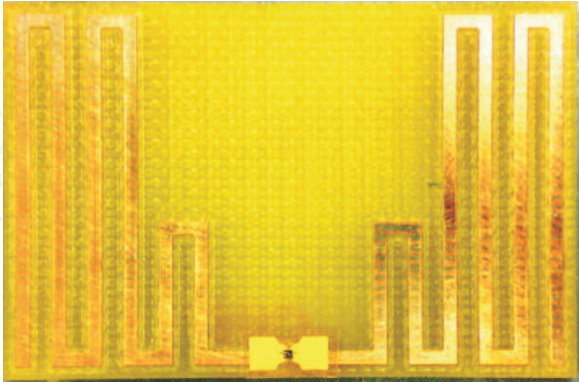


Fig. 6. A self-made tag used in experiment.

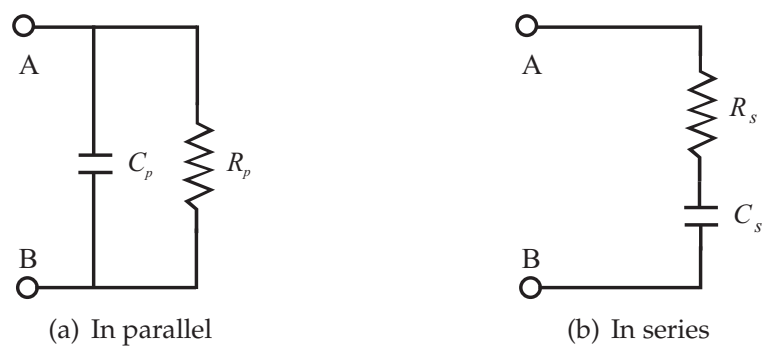


Fig. 7. The chip impedance illustration.

- *Reader*
The RFID reader used in the experiment is manufactured by FEIG Electronics which model is ID ISC.LRU2000. The reader antenna is the linearly polarised patch antenna with 8dBi gain and manufactured by Cushcraft Corporation, model: S9028P. The reason why the linearly polarised reader antenna is used is to simplify the model building in the simulation discussed later.
- *Shielding tunnel*
The reading range experiments were conducted by placing both the self-made tag and the reader antenna inside of a shielding tunnel. The size of the tunnel is $1826 \times 915 \times 690$ (unit mm), which is shown in Fig. 8. The shielding tunnel is surrounded by electromagnetic wave absorbing foam. The absorbing foam is manufactured by the Emerson & Cuming company for the frequency range from 600MHz to 4GHz. These absorbing foams can achieve maximum -22dB reflectivity around 1GHz. The inside space of the tunnel can thus be considered to be effectively free space.

As mentioned before, the reading range of the self-made tag were measured by placing the tag and the reader antenna in the shielding tunnel. Since the tunnel inside can be regarded as free space, it is not the complex environment as described in Subsection 7.3. In order to

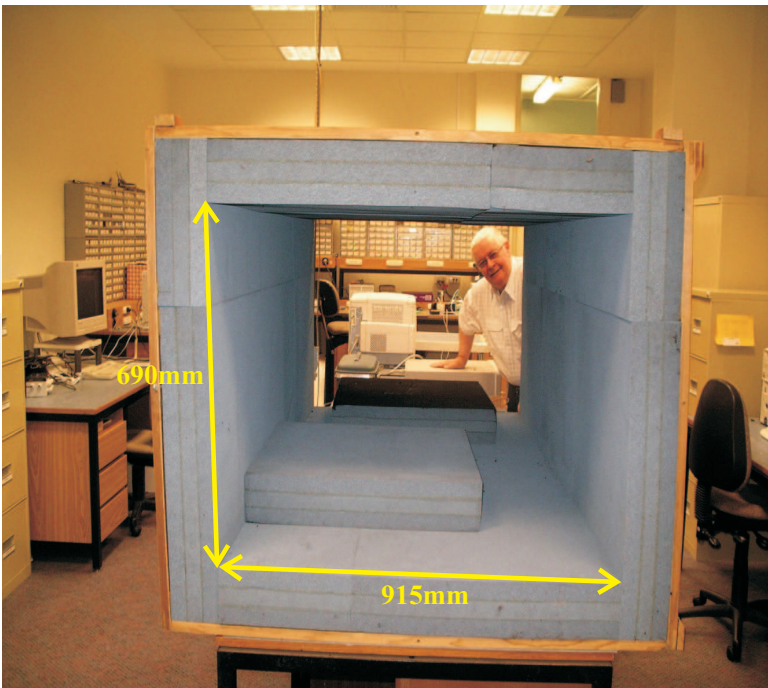


Fig. 8. A shielding tunnel.

make the environment complex, a square aluminium plate which length is 260mm is placed behind the tag. Various reading ranges of this tag were tested by varying the distance between the tag and the plate. The reading ranges are shown in Table 2. In Table 2, d_t is the distance between the tag and the aluminium plate. In the experiments d_t is formed by inserting one or two kinds of materials in slice between the tag and the plate. The materials are bubble wrap of which the thickness is 3mm and Teflon sheet of which the thickness is 0.97mm. It is believed that the effective permittivity of the bubble wrap is close to be 1. The relative permittivity of Teflon is usually about 2 with very low losses (Santra and Limaye, 2005; Plumb and MA, 1993). In order to minimise the effects of the Teflon, the Teflon sheet is cut into a much smaller footprint (6mm×8mm) than the tag. Given the low profile structure and small size, it is believed that the insertion of the Teflon sheet will not affect the results much either. The reading range tests were conducted by the equipment introduced before and under Australian UHF RFID regulations which frequency band is from 920MHz to 926MHz and the available source power of the reader generator is set to be 4W EIRP (36dBm). The reading range actually is the distance criterion after which the power received by the tag drops below its threshold power. In addition, the reading range of the tag in free space under the Australian regulations and tested by the equipment introduced before is about 5.2m.

d_t (mm)	3	4	5	6	7	8
Reading range (mm)	230	350	470	890	1000	1140

Table 2. Reading ranges of the self-made tag in proximity to the aluminium plate by experiments.

As illustrated by Table 2, the further the tag is away from the aluminium plate, the longer the reading range that is obtained. This phenomenon is easily understood since the metal beside will degrade the performance of the tag antenna. Then, the tag antenna, the aluminum plate behind the tag antenna and the reader antenna

were built in the simulation tool Ansoft HFSS. The two antennas’ terminals are connected to two lumped ports separately. In HFSS, such ports possess implied transmission line characteristic impedances. These lines could be connected to the ports and those lines allow scattering parameters to be defined.

In terms of the characteristic impedance, it can be set in HFSS as an arbitrary complex impedance. But, in reality the characteristic impedance of the transmission line between the reader antenna and the reader is 50Ω . As for the characteristic impedance of the transmission line between the tag antenna and the chip, it can be assumed to be any value, since its length is nearly zero, its characteristic impedance does not really matter. But, in order to get the symmetrical scattering matrix, it is set to be 50Ω as well in the simulation. In terms of source, since in reality the reader antenna is active and the tag antenna is passive, the lumped ports connected to the two antennas are therefore set to be an active port and a passive port respectively. In addition, the reader antenna in the simulation is not exactly the same to the one used in the experiment, since the reader antenna used in the experiment is a commercial antenna which is enclosed, so that the inside structure cannot be seen. But it is known that this commercial antenna design is based on a patch antenna. Hence, in the simulation we designed a patch antenna as the reader antenna with geometrical and electrical parameters similar to the one in the experiments.

After building, setting and simulating the model, the S parameters are derived directly at the two lumped ports. Furthermore, we have already known that the Higgs-2 chip’s impedance Z_{chip} at 923MHz is about $13.6-j142\Omega$ and the characteristic impedance Z_0 of the transmission line is 50Ω . Hence, inserting the derived S parameters, Z_{chip} and Z_0 into Equation 61, the power received by the chip at any relative distances among the aluminium plate, the tag and the reader antenna can be derived.

As mentioned before, as long as the communication between the reader and the tag is successful, the power received by the chip should be larger than the threshold power of the chip which is typically -14dBm. In other words, the longest reading range appears when the received power falls to -14dBm. Hence, in the simulation, the distance d_t between the aluminium plate and the tag, and the distance between the tag and the reader antenna will not stop varying until the power calculated by Equation 61 reaches -14dBm to get the longest reading range. The results are shown in Table 3.

d_t (mm)	3	4	5	6	7	8
Reading range (mm)	200	390	570	880	1040	1160

Table 3. Reading ranges of the self-made tag in proximity to the aluminium plate calculated by Equation 61 after deriving S parameters from the simulation.

In order to compare the data in Table 2 and Table 3, these results are plotted in Fig. 9. In Fig. 9, the x axis represents the distance between the tag and the aluminium plate. The y axis represents the reading range. The dashed curve comes from the experimental results which are given in Table 2 and the solid one comes from the calculated results by Equation 61 after deriving the S parameters from the simulation which are given in Table 3. The coincidence between the two curves validates Equation 61. It may be noticed that the differences between the two curves is relatively large when d_t is less than 6mm. This is because when d_t is small the reading range is very sensitive to the changes in d_t . In the simulation, d_t is exactly as the number you give to the simulation, but in the experiments, as we mentioned before, the distance d_t is formed by inserting the bubble wrap and Teflon sheet between the tag and the aluminum plate. The Teflon sheet is hard and its thickness at 0.97mm is very close to the 1mm

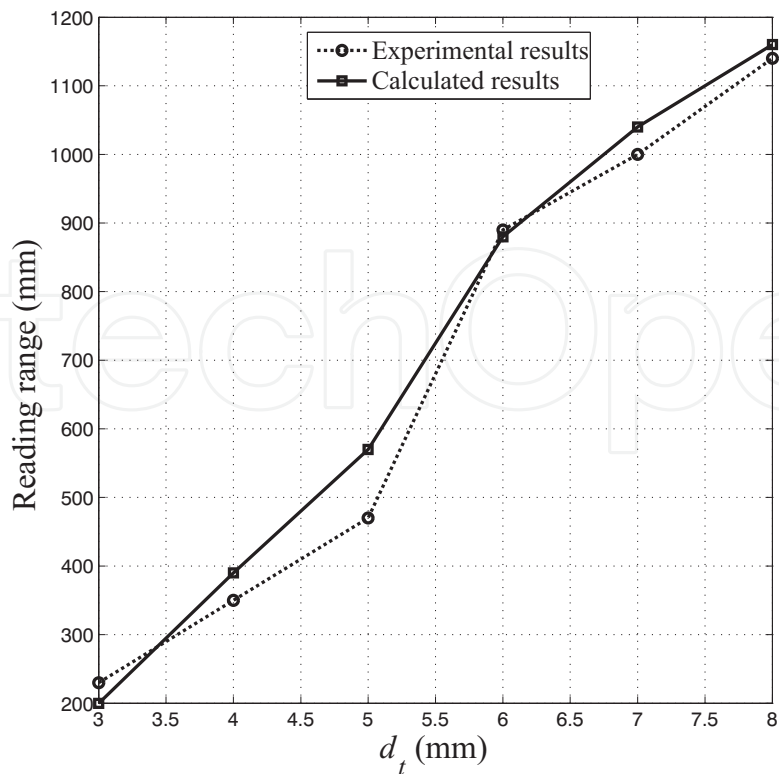


Fig. 9. Comparison between the reading range calculated by Equation 61 after deriving the S parameters from the simulation and the tested reading range.

assumed in the simulation. The thickness of the bubble wrap is about 3mm but it is soft and shape-flexible, hence the thickness may not be very accurately established. This may be the reason causing the error.

9. Conclusion

According to the discussion above, every aspect, e.g. the transponder IC design, the tag antenna design, the reader antenna design, and the deployed environment, in an RFID system affects the operating range of that system. Among all of them, there are a few factors which we believe play a significant role. (i) The selection of the parameter θ , the magnitude squared of which establishes the fraction of the available tag antenna power that is not delivered to the tag chip is one of the keys to lengthening the operating range, since it governs how much power would be delivered to power the chip and how much will be backscattered to sense the reader. (ii) The rectifier design is critical since the enhancement of the rectifier efficiency can lower the threshold power of the chip. (iii) The environment in which the system is deployed could be an obstacle in obtaining long operating range, especially when the environment involves many electro-magnetically sensitive materials surrounding the tags or even very close to the tag. Those materials include metal and water etc.

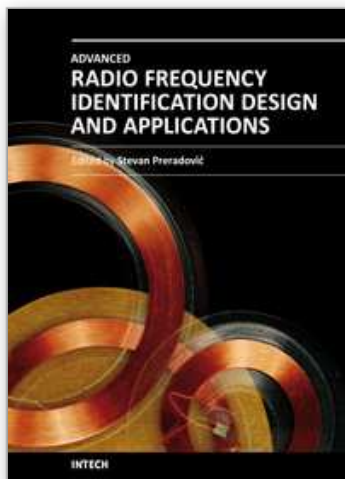
In addition, in this chapter, a novel method for evaluating the reading range of a UHF RFID system deployed in an arbitrary environment is proposed by means of a scattering matrix. The method is verified by experiments.

10. References

- [1] Alien Technology. Product overview of HiggsTM-2.
URL: http://www.alientechnology.com/docs/products/DS_H2.pdf
- [2] Balanis, C. A. (2005). *Antenna Theory*, 3rd ed., John Wiley, Hoboken, New Jersey.
- [3] Che, W.; Yan, N.; Yang, Y. & Hao, M. (2008). A low voltage, low power RF/analog front-end circuit for passive UHF RFID tags. *Chinese Journal of Semiconductors*, Vol. 29, No. 3, pp. 433–437, Mar. 2008.
- [4] Cole, P. H.; Turner, L.; Hu, Z. & Ranasinghe, D. (2010). The Future of RFID, In: *NUnique Radio Innovation for the 21st Century*, Ranasinghe, D.; Sheng, M. & Zeadally, S., (Ed.), Springer, 2010.
- [5] De Vita, G. & Iannaccone, G. (2005). Design criteria for the RF section of UHF and microwave passive RFID transponders. *IEEE Transactions on Microwave Theory and Techniques*, Vol. 53, No. 9, pp. 2978–2990, Sept. 2005.
- [6] Dobkin, D. & Weigand, S. (2005). Environmental effects on RFID tag antennas. *IEEE International Microwave Symposium Digest*, Vol. 5, No. 1, pp. 247–250, Jun. 2005.
- [7] Finkenzeller, K. (2003). *RFID handbook: fundamentals and applications in contactless smart cards and identification*, 2nd ed., John Wiley and Sons, ISBN: 9780470844021.
- [8] Fujitsu Microelectronics Limited. Ferroelectric RAM, *RFID Journal* Apr. 2006.
URL: www.fujitsu.com/downloads/EDG/binary/pdf/catalogs/a05000249e.pdf
- [9] Fuschini, F.; Piersanti, C.; Paolazzi, F.; & Falciasacca, G. (2008). Electromagnetic and System Level Co-Simulation for RFID Radio Link Modeling in Real Environment. *The Second European Conference on Antennas and Propagation*, pp. 1–8, Nov. 2007.
- [10] Fuschini, F.; Piersanti, C.; Paolazzi, F.; & Falciasacca, G. (2008). Analytical Approach to the Backscattering from UHF RFID Transponder. *IEEE Antennas and Wireless Propagation Letters*, Vol. 7, pp. 33–35, 2008.
- [11] Griffin, J.; Durgin, G.; Haldi, A. & Kippelen, B. (2003). RF Tag Antenna Performance on Various Materials Using Radio Link Budgets. *IEEE Antennas and Wireless Propagation Letters*, Vol. 5, No. 1, pp. 247–250, Dec. 2006.
- [12] Hodges, S.; Thorne, A.; Mallinson, H. & Floerkemeier, C. (2007). Assessing and optimizing the range of UHF RFID to enable real-world pervasive computing applications. *Proceedings of the 5th international conference on Pervasive computing*, 2007.
- [13] Jiang, B.; Fishkin, K.; Roy, S. & Philipose, M. (2006). Unobtrusive long-range detection of passive RFID tag motion. *IEEE Transactions on Instrumentation and Measurement*, Vol. 55, No. 1, pp. 187–196, Feb. 2006.
- [14] Karthaus, U. & Fischer, M. (2003). Fully integrated passive UHF RFID transponder IC with 16.7 μ W minimum RF input power. *IEEE Journal of Solid-State Circuits*, Vol. 38, No. 10, pp. 1602–1608, Oct. 2003.
- [15] Leong, K. S. (2008). Antenna position analysis and dual-frequency antenna design of high frequency ratio for advanced electronic code responding labels, Ph.D. dissertation, The University of Adelaide, Adelaide, Australia.
- [16] Lung, H. L.; Lai, S.; Lee, H.; Wu, T. B.; Liu, R. & Lu, C. Y. (2004). Low-temperature capacitor-overinterconnect (COI) modular FeRAM for SOC application. *IEEE Transactions on Electron Devices*, Vol. 51, No. 6, pp. 920–926, Jun. 2004.
- [17] Nakamoto, H.; Yamazaki, D.; Yamamoto, T.; Kurata, H.; Yamada, S.; Mukaida, K.; Ninomiya, T.; Ohkawa, T.; Masui, S. & Gotoh, K. (2007). A passive UHF RF identification CMOS tag IC using ferroelectric RAM in 0.35 μ m technology. *IEEE Journal of Solid-State Circuits*, Vol. 42, No. 1, pp. 101–110, Jan. 2007.

- [18] NG, M. L. (2008). Design of high performance RFID system for metallic item identification, Ph.D. dissertation, The University of Adelaide, Adelaide, Australia.
- [19] Nikitin, P. & Rao, K. (2006). Performance limitations of passive UHF RFID systems. *IEEE Antennas and Propagation Society International Symposium*, pp. 1011–1014, Jul. 2006.
- [20] Nikitin, P. & Rao, K. (2006). Theory and measurement of backscattering from RFID tags. *IEEE Antennas and Propagation Magazine*, Vol. 48, No. 6, pp. 212–218, Dec. 2006.
- [21] No author stated. The Cost of RFID Equipment, *RFID Journal*.
URL: www.rfidjournal.com/faq/20
- [22] Plumb, R. & Ma, H. (1993). Swept frequency reflectometer design for in-situ permittivity measurements. *IEEE Transactions on Instrumentation and Measurement*, Vol. 42, No. 3, pp. 730–734, Jun. 1993.
- [23] Prothro, J.; Durgin, G. & Griffin, J. (2005). The effects of a metal ground plane on RFID tag antennas. *IEEE Antennas and Propagation Society International Symposium*, pp. 3241–3244, Jul. 2006.
- [24] Rappaport, T. (2002). *Wireless communications-principles and practice*, 2nd ed., Prentice Hall.
- [25] Santra, M. & Limaye, K. (2005). Estimation of complex permittivity of arbitrary shape and size dielectric samples using cavity measurement technique at microwave frequencies. *IEEE Transactions on Microwave Theory and Techniques*, Vol. 53, No. 2, pp. 718–722, Feb. 2005.
- [26] Young, P. H. (1994). *Electronic Communication Techniques*, 3rd ed., Merrill, New York.
- [27] 3M. Conductive Adhesive Transfer Tape 9703 (Data Sheet).
URL: multimedia.3m.com/mws/mediawebserver?mwsId=66666UuZjcFSLXTtnxf VMxz 6E VuQEcuZgVs6EVs6E666666–

IntechOpen



Advanced Radio Frequency Identification Design and Applications

Edited by Dr Stevan Preradovic

ISBN 978-953-307-168-8

Hard cover, 282 pages

Publisher InTech

Published online 22, March, 2011

Published in print edition March, 2011

Radio Frequency Identification (RFID) is a modern wireless data transmission and reception technique for applications including automatic identification, asset tracking and security surveillance. This book focuses on the advances in RFID tag antenna and ASIC design, novel chipless RFID tag design, security protocol enhancements along with some novel applications of RFID.

How to reference

In order to correctly reference this scholarly work, feel free to copy and paste the following:

Peter. H. Cole, Zhonghao Hu and Yuexian Wang (2011). Operating Range Evaluation of RFID Systems, Advanced Radio Frequency Identification Design and Applications, Dr Stevan Preradovic (Ed.), ISBN: 978-953-307-168-8, InTech, Available from: <http://www.intechopen.com/books/advanced-radio-frequency-identification-design-and-applications/operating-range-evaluation-of-rfid-systems>

INTECH
open science | open minds

InTech Europe

University Campus STeP Ri
Slavka Krautzeka 83/A
51000 Rijeka, Croatia
Phone: +385 (51) 770 447
Fax: +385 (51) 686 166
www.intechopen.com

InTech China

Unit 405, Office Block, Hotel Equatorial Shanghai
No.65, Yan An Road (West), Shanghai, 200040, China
中国上海市延安西路65号上海国际贵都大饭店办公楼405单元
Phone: +86-21-62489820
Fax: +86-21-62489821

© 2011 The Author(s). Licensee IntechOpen. This chapter is distributed under the terms of the [Creative Commons Attribution-NonCommercial-ShareAlike-3.0 License](https://creativecommons.org/licenses/by-nc-sa/3.0/), which permits use, distribution and reproduction for non-commercial purposes, provided the original is properly cited and derivative works building on this content are distributed under the same license.

IntechOpen

IntechOpen